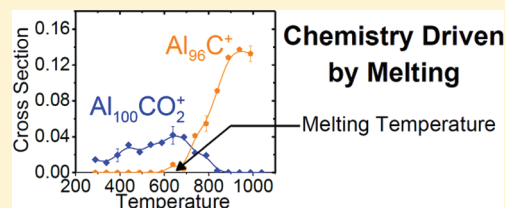


Reactions of CO₂ on Solid and Liquid Al₁₀₀⁺

Katheryne L. Leslie, Deven Shinholt, and Martin F. Jarrold*

Chemistry Department, Indiana University, 800 E. Kirkwood Avenue, Bloomington, Indiana 47405, United States

ABSTRACT: The reactions of CO₂ on the Al₁₀₀⁺ cluster have been investigated as a function of cluster temperature (300–1100 K) and relative kinetic energy (0.2–10 eV). Two main products are observed at low cluster temperature: Al₁₀₀O⁺ (which is believed to result from a stripping reaction) and Al₁₀₀CO₂⁺ from complex formation. As the cluster temperature is raised, both products dissociate by loss of Al₂O. Al₁₀₀O⁺ forms Al₉₈⁺, while Al₁₀₀CO₂⁺ forms Al₉₈CO⁺ and Al₉₆C⁺. In both cases, loss of Al₂O turns-on above the melting temperature of Al₁₀₀⁺. This presumably occurs because the overall reaction leading to the loss of Al₂O is significantly less endothermic for the liquid cluster than for the solid.

Chemistry Driven
by Melting

■ INTRODUCTION

Not much is known about the chemical properties of liquid metals. For solid metals, the structure of the surface (the orientation and the presence of steps and defects) affects reactivity.¹ The surfaces of many liquid metals are layered with a short-range order that extends several atomic layers.^{2–4} The difference between the structures of the liquid and solid surfaces probably means that they have different chemical properties, at least for processes that are sensitive to surface structure. The dynamic properties of liquids are also different from those of the corresponding solids. Processes that require the surface to move so that reagents can become embedded before a reaction occurs, and processes that result in strain, may be enhanced at a liquid surface. Similarly, some reactions may be driven by the dissolution of the products into the liquid metal.

Metal clusters provide a useful vehicle to study the effects of melting on chemical reactivity. Clusters usually have depressed melting temperatures, and there are often large size-dependent fluctuations, so that some cluster sizes have melting points that are much lower than the bulk value. Our group has recently reported measurements of the kinetic energy thresholds for chemisorption of N₂ onto Al₄₄[±] and Al₁₀₀⁺ as a function of cluster temperature.^{5,6} We found that the kinetic energy threshold for chemisorption was around 3 eV on the solid clusters but dropped to around 2 eV when the clusters melt. This 1 eV drop in the kinetic energy threshold translates into a 10⁸-fold increase in the reaction rate. So in this case, the liquid cluster is much more reactive than the solid.

The melting temperatures for isolated aluminum clusters have been determined from heat capacity measurements performed as a function of temperature.^{7–9} A peak in the heat capacity due to the latent heat is used to identify the melting point. Most aluminum clusters melt significantly below the bulk melting point of 934 K. A melting point depression is expected for small particles.¹⁰ In the case of Al₁₀₀⁺, a maximum in the heat capacity centered at around 639 K has been assigned to the melting transition.¹¹ The melting transition for Al₁₀₀⁺ is around 80–90 K wide. Liquid and solid Al₁₀₀⁺ clusters coexist

in a dynamic equilibrium over this temperature range.¹² This behavior is different from the melting of a macroscopic aluminum sample, which occurs at a single temperature (934 K). The broadening of the melting transition is a well-known effect of the cluster's small size.^{13,14} The width of the melting transition for aluminum clusters appears to be correlated with their latent heat.¹⁵ Al₁₀₀⁺ has a relatively large latent heat (small width) compared to other aluminum clusters in the same size regime. The origin of the large latent heat is not known, it presumably reflects the properties of the solid cluster (i.e., a particularly stable or well-organized structure) because it is difficult to imagine that the liquid clusters have properties that are strongly size dependent.

While metal clusters provide a useful vehicle to study the effect of phase on chemical reactivity, it is important to recognize that liquid metal clusters may have properties that differ from the corresponding macroscopic liquids. For example, thin liquid films show a quantized response to shear forces.¹⁶ While thin liquid films are confined in one dimension, liquid clusters are confined in all three dimensions. Not much is known about the physical properties of liquid clusters, though one might expect that they are more ordered than the surfaces of liquid metals.

The origin of the decrease in the activation energy for N₂ chemisorption on Al₄₄[±] that occurs when the cluster melts has been investigated using density functional calculations.⁶ The strong increase in reactivity on melting appears to be due to the volume change of melting and to atomic disorder. As a result of the thermal expansion that occurs upon melting, the mobile atoms of a liquid cluster can minimize their energy to better accommodate the incoming reagent and decrease the activation energy.

In this article, we report studies of the chemisorption of CO₂ on Al₁₀₀⁺ as a function of relative kinetic energy and cluster

Special Issue: Peter B. Armentrout Festschrift

Received: April 5, 2012

Revised: May 23, 2012

Published: June 11, 2012

temperature. We selected Al_{100}^+ for these studies because this cluster has a sharp, well-defined melting transition. It is also large enough that the properties are not strongly size dependent. On the negative side, there is little information available on the structure of Al_{100}^+ .¹⁷ CO_2 is usually considered inert¹⁸ because of the large bond energy of each carbon–oxygen bond (around 800 kJ/mol¹⁹). However, a number of investigations of the interaction between carbon dioxide and metal surfaces, including aluminum, have been performed.^{20,21} It has been found that CO_2 is usually physisorbed at low temperatures and then often dissociatively chemisorbs upon warming.

EXPERIMENTAL METHODS

The experiments were performed using a home-built instrument that has been described in detail elsewhere.^{6,22} The clusters are formed by laser vaporization of a liquid aluminum target in a helium buffer gas. Use of a liquid target increases the intensity and stability of the signal compared to that obtained with a solid target.²³ Cluster ions formed in the source region are carried by the buffer gas flow into a 10 cm long temperature-variable extension where they undergo enough collisions with buffer gas to be equilibrated to the temperature of the walls. The temperature of the extension is regulated to ± 2 K by a programmable microprocessor-based temperature controller. Upon exiting the extension, the cluster ions are accelerated and focused into a quadrupole mass spectrometer (Extrel, Pittsburgh, PA) where a single cluster size is selected.

The cluster ions that are transmitted by the quadrupole are focused into a low energy ion beam and passed through a low-pressure reaction cell. The kinetic energy of the cluster ions in the reaction cell is determined from the potential difference between the reaction cell and the source. The pressure of the reagent in the reaction cell is kept low (usually around 0.3 mTorr) to minimize multiple collisions. A few experiments were performed as a function of reagent pressure to investigate whether some of the products resulted from multiple collisions.

Product and parent ions that exit the reaction cell are focused into a second quadrupole mass spectrometer where they are mass analyzed and then detected with an off-axis collision dynode and dual microchannel plates (Photonis, Sturbridge, MA). Signals from the detector are amplified and transmitted to a computer where they are accumulated as the quadrupole is scanned.

The product ions exiting the collision cell have a range of kinetic energies. The kinetic energy of a given product ion is determined primarily by the mass lost or gained in the reaction. Because the range of product ion masses is relatively large in the work reported here, there is the possibility of discrimination in the focusing of the ions into the second quadrupole mass spectrometer and in the transmission of the ions through this quadrupole. In order to avoid discrimination, the quadrupole bias voltage and one of the voltages on the electrostatic lens between the collision cell and the quadrupole are adjusted as the mass transmitted by the second quadrupole is scanned. A LabVIEW program controls the focusing lens voltage, the quadrupole bias voltage, and the quadrupole mass command. Three data acquisition cards are utilized to perform these functions and accumulate the signal from the detector: a USB-4302 counter/timer and two PCI-2517 multifunction digital acquisition cards (Measurement Computing, Norton, MA). SIMION simulations were performed to generate algorithms to set the focusing voltage and quadrupole bias voltage.

A Fortran program is used to subtract baseline noise from the measured mass spectra and integrate peaks according to a user-defined list of peak boundaries.

EXPERIMENTAL RESULTS

Two types of experiments were performed. In the first, we fixed the cluster temperature and measured reaction cross-sections as a function of collision energy; and in the second, we fixed the collision energy and performed measurements as a function of the cluster temperature. The total reaction cross-section was obtained from

$$\sigma = \ln \left[\frac{I_R + \sum I_p}{I_R} \right] \frac{1}{Nl} \quad (1)$$

where I_R is intensity of the remaining, unreacted ions, I_p are the intensities of the product ions determined from the measured mass spectrum, N is the neutral reagent number density, and l is the length of the reaction cell. Figure 1 shows the cross-

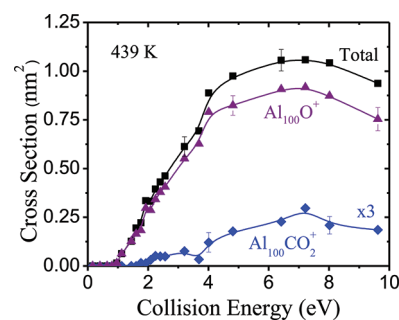
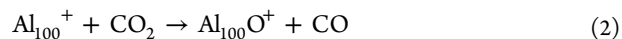


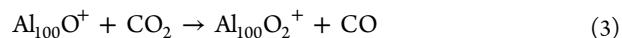
Figure 1. Plot of the total cross-sections and the cross-sections for the main single collision products ($\text{Al}_{100}\text{O}^+$ and $\text{Al}_{100}\text{CO}_2^+$) from the reaction of CO_2 with Al_{100}^+ with a cluster temperature of 439 K. Error bars show the estimated uncertainties.

sections measured for the reaction between Al_{100}^+ and CO_2 for a range of collision energies with an initial cluster temperature of 439 K. This temperature is 200 K below the melting temperature of Al_{100}^+ . Three main products are observed: $\text{Al}_{100}\text{O}^+$, $\text{Al}_{100}\text{O}_2^+$, and $\text{Al}_{100}\text{CO}_2^+$. The total reaction cross-section shown in Figure 1 has a kinetic energy threshold at approximately 1 eV. For kinetic energies above the threshold, the total cross-sections increase roughly linearly with the collision energy until they plateau at around 1.0 nm^2 near 6 eV. At the higher collision energies the cross-sections begin to decrease.

Cross-sections measured for the individual products are also shown in Figure 1. The most abundant product observed with a cluster temperature of 439 K is from the addition of a single oxygen atom, which presumably occurs through the reaction

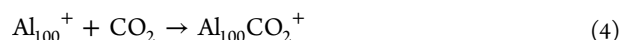


The cross-sections for this product follow the same trend as the total cross-section. In addition to the $\text{Al}_{100}\text{O}^+$ product, a small amount of $\text{Al}_{100}\text{O}_2^+$ was observed. Measurements performed as a function of the reagent pressure showed that the $\text{Al}_{100}\text{O}_2^+$ product results from a two collision process where the $\text{Al}_{100}\text{O}^+$ product presumably reacts with a second CO_2 molecule according to the equation



We do not include the results for the $\text{Al}_{100}\text{O}_2^+$ product in Figure 1 since this product results from a two collision process. However, this product is included in the total cross-sections.

The other significant product observed with a cluster temperature of 439 K is from the addition of a CO_2 molecule as follows:



Cross-sections for this process are plotted in Figure 1. The cross-sections for the $\text{Al}_{100}\text{CO}_2^+$ product are much smaller than for the $\text{Al}_{100}\text{O}^+$ product. There is a kinetic energy threshold associated with formation of the $\text{Al}_{100}\text{CO}_2^+$ product at a slightly higher kinetic energy than the threshold for the $\text{Al}_{100}\text{O}^+$ product.

Cross-sections measured for the reactions between Al_{100}^+ and CO_2 with an initial cluster temperature of 717 K are shown in Figure 2. This temperature is around 80 K above the melting

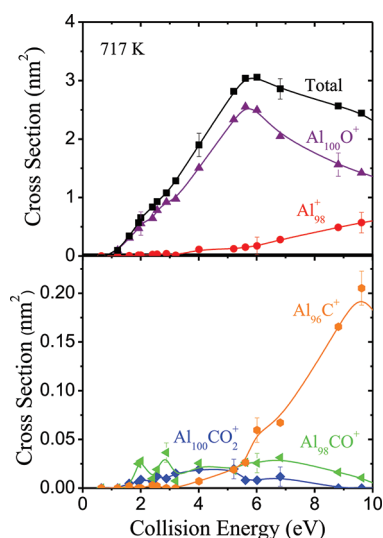


Figure 2. Plot of the total cross-sections and the cross-sections for the main single collision products from the reaction of CO_2 with Al_{100}^+ with a cluster temperature of 717 K. Cross-sections for $\text{Al}_{100}\text{O}^+$ and its secondary product Al_{98}^+ are shown in the top panel. Cross-sections for $\text{Al}_{100}\text{CO}_2^+$ and its secondary products $\text{Al}_{98}\text{CO}^+$ and Al_{96}C^+ are shown in the lower panel. Error bars show the estimated uncertainties.

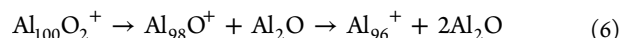
temperature of Al_{100}^+ . The total cross-section shows a threshold that is at approximately the same kinetic energy as found with an initial cluster temperature of 439 K. The total cross-sections rise and reach a peak at around 6 eV, before decreasing. The peak cross-section of around 3.0 nm^2 is significantly larger than observed at 439 K.

In addition to the products observed at 439 K ($\text{Al}_{100}\text{O}^+$, $\text{Al}_{100}\text{O}_2^+$, and $\text{Al}_{100}\text{CO}_2^+$), a number of other products are observed at 717 K, including Al_{98}^+ , Al_{98}O^+ , Al_{96}^+ , $\text{Al}_{98}\text{CO}^+$ / Al_{99}^+ , Al_{96}C^+ , Al_{95}^+ , Al_{94}C^+ , and Al_{94}^+ . The dominant product observed at the lower collision energies is $\text{Al}_{100}\text{O}^+$. At higher collision energies, Al_{98}^+ becomes an important product. It is likely that this product results from the loss of Al_2O from $\text{Al}_{100}\text{O}^+$ according to



Al_2O is known to be a stable species,²⁴ and it is an inferred product in the reactions between smaller aluminum clusters and O_2 .²⁵ A small amount of $\text{Al}_{100}\text{O}_2^+$ is observed from the

reaction of $\text{Al}_{100}\text{O}^+$ with a second CO_2 molecule. At high collision energies, Al_{98}O^+ and Al_{96}^+ are observed as minor products. We attribute these species to the sequential loss of two Al_2O molecules from $\text{Al}_{100}\text{O}_2^+$ as follows:



Addition of CO_2 to the cluster leads to $\text{Al}_{100}\text{CO}_2^+$ as a minor product. We connect this product with two other minor products: $\text{Al}_{98}\text{CO}^+$ and Al_{96}C^+ . Al_{96}C^+ becomes a significant product at high kinetic energies (see Figure 2). We attribute this product to the sequential loss of two Al_2O molecules from $\text{Al}_{100}\text{CO}_2^+$ according to



The mass of the $\text{Al}_{98}\text{CO}^+$ product is similar to the mass of Al_{99}^+ . Our mass resolution is insufficient to resolve these species, so we cannot rule out the presence of some Al_{99}^+ , which could, for example, result from collision-induced dissociation of Al_{100}^+ . There are several more minor products (including Al_{95}^+ , Al_{94}C^+ , and Al_{94}^+), which we do not discuss further here.

Cross-sections measured with an initial cluster temperature of 1049 K are shown in Figure 3. This temperature is around

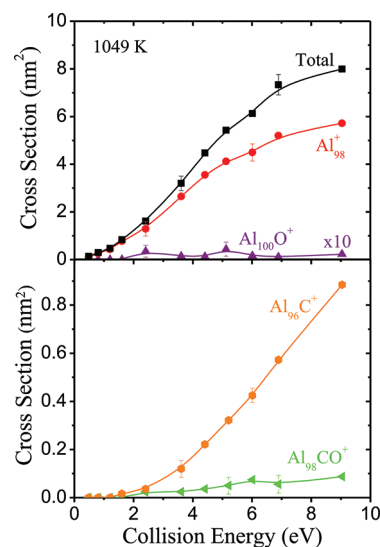


Figure 3. Plot of the total cross-sections and the cross-sections for the main single collision products from the reaction of CO_2 with Al_{100}^+ with a cluster temperature of 1049 K. Cross-sections for $\text{Al}_{100}\text{O}^+$ and its secondary product Al_{98}^+ are shown in the top panel. Cross-sections for $\text{Al}_{98}\text{CO}^+$ and Al_{96}C^+ (secondary products from $\text{Al}_{100}\text{CO}_2^+$) are shown in the lower panel. Error bars show the estimated uncertainties.

410 K above the melting temperature of Al_{100}^+ . The products observed at 1049 K are similar to those found at 717 K. The kinetic energy threshold is shifted to slightly lower kinetic energies than at 717 K. The threshold also seems to be broader than at the lower temperatures. The total cross-sections rise continuously as the collision energy increases, reaching around 8 nm^2 at a collision energy of 10 eV. This behavior contrasts with that found at lower temperatures where there is a peak in the total cross-sections at lower collision energies. The total cross-sections found at the lower temperatures are also significantly smaller than at 1049 K.

The dominant product at 1049 K is Al_{98}^+ , which, on the basis of the results at lower temperatures, probably results from loss of Al_2O from $\text{Al}_{100}\text{O}^+$. $\text{Al}_{100}\text{O}^+$ is present as a minor product at

1049 K. Al_{96}^+ is also present as a minor product. This product probably results from the loss of two Al_2O molecules from the two-collision product $\text{Al}_{100}\text{O}_2^+$.

The $\text{Al}_{100}\text{CO}_2^+$ product from the addition of CO_2 was not observed at 1049 K. However, the fragmentation products of $\text{Al}_{100}\text{CO}_2^+$ identified at lower temperatures, $\text{Al}_{98}\text{CO}^+$ and Al_{96}C^+ , are observed (see Figure 3). The thresholds for these products are at a significantly higher kinetic energy than the threshold for the Al_{98}^+ product.

For the second set of experiments mentioned above, the collision energy was fixed at 4 eV, and measurements were performed as a function of cluster temperature ranging from 289 to 1039 K in increments of 50 K. The results of these measurements are shown in Figure 4. At low temperatures, the

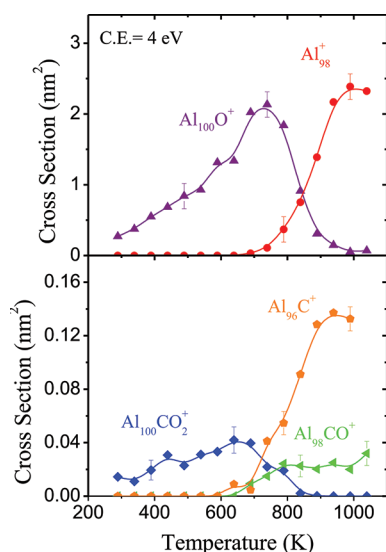


Figure 4. Plot of the cross-sections measured for the main single collision products from the reaction between CO_2 and Al_{100}^+ as a function of cluster temperature. The collision energy was 4 eV. Error bars show the estimated uncertainties.

dominant product is $\text{Al}_{100}\text{O}^+$. Starting at around 700 K, the cross-section for the $\text{Al}_{100}\text{O}^+$ product decreases and the cross-section for the Al_{98}^+ product increases. These results are consistent with the view that the Al_{98}^+ product results from loss of Al_2O from $\text{Al}_{100}\text{O}^+$. Note that the $\text{Al}_{100}\text{O}^+$ product starts to decrease and the Al_{98}^+ product starts to increase at around 700 K (just above the melting temperature of the Al_{100}^+ cluster at 639 K). The cross-sections for the $\text{Al}_{100}\text{CO}_2^+$, $\text{Al}_{98}\text{CO}^+$, and Al_{96}C^+ products are shown in the lower panel of Figure 4. The appearance of these products is consistent with the view that the Al_{96}C^+ product results from the loss of two Al_2O molecules from $\text{Al}_{100}\text{CO}_2^+$. Below the melting temperature of Al_{100}^+ , only the addition product is observed. Note that the increase in the $\text{Al}_{98}\text{CO}^+$ and Al_{96}C^+ products occurs at roughly the same temperature as the increase in the Al_{98}^+ product.

DISCUSSION

Two main products are observed in the reaction between Al_{100}^+ and CO_2 at the lowest temperature studied (439 K): $\text{Al}_{100}\text{O}^+$ and $\text{Al}_{100}\text{CO}_2^+$. The fact that the $\text{Al}_{100}\text{CO}_2^+$ complex survives at 439 K indicates that the CO_2 must be chemisorbed onto the Al_{100}^+ cluster. A weakly bound, physisorbed CO_2 would not remain bound to the Al_{100}^+ cluster long enough to be detected at 439 K.

Both of the main products observed at 439 K ($\text{Al}_{100}\text{O}^+$ and $\text{Al}_{100}\text{CO}_2^+$) show a kinetic energy threshold. A kinetic energy threshold usually indicates the presence of an activation barrier at some point along the reaction coordinate. The threshold for $\text{Al}_{100}\text{CO}_2^+$ is significantly larger than for formation $\text{Al}_{100}\text{O}^+$. This indicates that formation of the $\text{Al}_{100}\text{CO}_2^+$ complex is not a precursor to formation of $\text{Al}_{100}\text{O}^+$. The $\text{Al}_{100}\text{O}^+$ must be formed by a more direct reaction, perhaps a stripping reaction in which the metal cluster strips away an oxygen atom from a passing CO_2 , leaving the trajectory of the other two atoms (the remaining CO) largely unaffected. Stripping reactions have been well-characterized through the pioneering work of Mahan, Herman, and Lee.^{26–28}

The fact that there is a kinetic energy threshold associated with the formation of the $\text{Al}_{100}\text{CO}_2^+$ complex provides further evidence that the CO_2 is chemisorbed. However, the measurements reported here provide no information about the nature of the $\text{Al}_{100}\text{CO}_2^+$ complex and whether the CO_2 is chemisorbed intact or dissociatively chemisorbed.

In XPS studies of the interaction of CO_2 with polycrystalline aluminum, it was found that CO_2 physisorbs at low temperature (80 K).^{29,30} Upon warming to 120 K, the physisorbed CO_2 converts into a surface carbonate (this process presumably results from dissociation of some of the CO_2 to yield surface CO and O). The surface carbonate dissociates between 200 and 300 K to yield carbon (both graphitic and carbide) and O^{2-} . While the CO_2 molecule is clearly dissociated in the $\text{Al}_{96}\text{C}^+ + 2\text{Al}_2\text{O}$ products, our measurements do not provide information on when dissociation occurs.

There is a kinetic energy threshold for chemisorption of CO_2 on the Al_{100}^+ cluster, while dissociative chemisorption occurs on the surface below room temperature. The initial steps in the chemisorption of CO_2 are believed to involve electron transfer from the metal surface to the CO_2 , and a low work function is thought to promote dissociative chemisorption of CO_2 .²¹ The positive charge on the Al_{100}^+ cluster will make electron transfer to the CO_2 less favorable, and this is probably responsible for the kinetic energy threshold.

The kinetic energy threshold for $\text{Al}_{100}\text{O}^+$ formation is at around 1 eV for cluster temperatures of both 439 and 717 K. Similarly, the kinetic energy thresholds for $\text{Al}_{100}\text{CO}_2^+$ formation are at around 1.5 eV for both 439 and 717 K. At 439 K, the Al_{100}^+ cluster is solid-like, while at 717 K, it is liquid-like; so the kinetic energy thresholds for both reactions are not significantly affected by the melting transition. We did not attempt to extract accurate values for the kinetic energy thresholds from the measurements because the thresholds measured above and below the melting temperature are not significantly different. At a cluster temperature of 1049 K, the thresholds for both reactions are broader and appear to be shifted to somewhat lower kinetic energies. The lowering of the kinetic energy thresholds is probably due to the additional internal energy in the clusters at the higher temperature. The insensitivity of the kinetic energy thresholds to the phase of the cluster is in contrast to the behavior found for the reactions with N_2 where the threshold decreases by around 1 eV when the cluster melts.^{5,6} Above, we suggested that the reaction leading to $\text{Al}_{100}\text{O}^+$ occurs through a direct process, and this may explain why it is insensitive to the phase of the cluster. It is less obvious why the kinetic energy threshold for the chemisorption process leading to $\text{Al}_{100}\text{CO}_2^+$ is insensitive to the phase when chemisorption of N_2 on Al_{100}^+ depends strongly on the phase.

Below the melting temperature of Al_{100}^+ (639 K), the only single collision products that are observed are $\text{Al}_{100}\text{O}^+$ and $\text{Al}_{100}\text{CO}_2^+$ (see Figures 1 and 4). However, above the melting temperature, products that appear to result from the loss of Al_2O from $\text{Al}_{100}\text{O}^+$ and $\text{Al}_{100}\text{CO}_2^+$ become dominant. The loss of Al_2O from $\text{Al}_{100}\text{O}^+$ yields Al_{98}^+ . It is tempting to assume that $\text{Al}_{100}\text{O}^+$ is an intermediate in the overall reaction



However, we should mention the other possibility, which is that the reaction mechanism changes when the Al_{100}^+ melts, so that the loss of Al_2O is linked directly to the transfer of an oxygen atom from CO_2 . There is, however, no evidence to support this change. From the results shown in Figure 4, the amounts of the $\text{Al}_{100}\text{O}^+$ and Al_{98}^+ products are closely correlated above the melting temperature of Al_{100}^+ . This observation is more in tune with the idea that $\text{Al}_{100}\text{O}^+$ is an intermediate.

If $\text{Al}_{100}\text{O}^+$ is an intermediate, then we need to consider whether the melting temperature of $\text{Al}_{100}\text{O}^+$ is likely to be significantly different from that of Al_{100}^+ . Al_{100}^+ is sufficiently large that it is in a size regime where the melting temperatures change smoothly with cluster size. Hock et al. have reported a small systematic melting point depression (17 ± 6 K) following the addition of an oxygen molecule (O_2) to sodium clusters with 135–192 atoms.³¹ The melting point depression scales with the number of oxygen molecules added to the clusters. On the basis of these observations, we expect the melting temperature of $\text{Al}_{100}\text{O}^+$ to be slightly lower than for that of Al_{100}^+ .

There is enough information available to estimate the energetics of the overall reaction shown in eq 8. The energy required to remove a single aluminum atom from an aluminum cluster depends on whether the cluster is liquid or solid. Dissociation energies of metal clusters are usually measured by providing enough energy to cause dissociation and then taking into account the finite lifetime of the excited cluster using a statistical model. For larger clusters, dissociation is expected to occur from a liquid cluster to yield a liquid cluster product:¹⁵



The dissociation energy determined from this scheme is for the liquid cluster. The dissociation energy of the solid cluster is given by¹⁵

$$D_s(n) = D_l(n) + L^\circ(n) - L^\circ(n-1) \quad (10)$$

where $D_l(n)$ is the dissociation energy of the liquid cluster with n atoms (i.e., the average energy required to remove one atom from the liquid cluster), and $L^\circ(n)$ and $L^\circ(n-1)$ are the latent heats of fusion for the n -atom cluster and the $(n-1)$ -atom clusters, respectively. Dissociation energies measured for liquid aluminum clusters are insensitive to cluster size. The energy required to remove an aluminum atom from liquid clusters in the size range examined here is around 290 kJ/mol.¹⁵ Using this value, along with $D(\text{CO}-\text{O})$ (532 kJ/mol) and the dissociation energy of Al_2O (1042 kJ/mol)²⁴ yields an enthalpy change of around 70 kJ/mol for the reaction represented by eq 8. For the solid cluster, the enthalpy change increases to around 250 kJ/mol because the energy to remove two aluminum atoms from the solid Al_{100}^+ cluster is larger than for the liquid cluster (due to the latent heats in eq 10). So the overall reaction represented by eq 8 is considerably less endothermic on the liquid cluster than on the solid. This may explain why the loss

of Al_2O from $\text{Al}_{100}\text{O}^+$ occurs above the cluster melting temperature.

Loss of Al_2O from the $\text{Al}_{100}\text{CO}_2^+$ complex also occurs above the Al_{100}^+ melting temperature. In this case, up to two Al_2O molecules are lost leaving behind Al_{96}C^+ . It is likely that the lower endothermicity of the overall reaction on the liquid clusters compared to the solid, also provides an explanation for why loss of Al_2O from $\text{Al}_{100}\text{CO}_2^+$ does not occur below the Al_{100}^+ melting temperature.

In the results shown in Figure 4, both Al_2O molecules appear to evaporate from the $\text{Al}_{100}\text{CO}_2^+$ at close to the same temperature. If the cluster was a macroscopic object and both Al_2O molecules occupied identical, noninteracting sites, they would both evaporate at the same temperature. For the finite-sized cluster, evaporation of the first Al_2O will cool the cluster slightly, so that a slightly higher temperature should be required to evaporate the second. The fact that both Al_2O molecules appear to evaporate at the same temperature may indicate that the second Al_2O is slightly less strongly bound than the first. Thus, there may be a small cooperative effect in the binding of the Al_2O molecules. Such a cooperative effect would require that the nascent Al_2O molecules are close enough to interact in the $\text{Al}_{100}\text{CO}_2^+$ cluster

AUTHOR INFORMATION

Corresponding Author

*E-mail: mfj@indiana.edu.

Notes

The authors declare no competing financial interest.

ACKNOWLEDGMENTS

We gratefully acknowledge the support of the National Science Foundation through grant number 0911462.

REFERENCES

- (1) Somorjai, G. A. *Chemistry in Two Dimensions: Surfaces*; Cornell University Press: Ithaca, NY, 1981.
- (2) D'Evelyn, M. P.; Rice, S. A. *Phys. Rev. Lett.* **1981**, *47*, 1844–1847.
- (3) Regan, M. J.; Kawamoto, E. H.; Lee, S.; Pershan, P. S.; Maskil, N.; Ocko, B. M.; Berman, L. E. *Phys. Rev. Lett.* **1995**, *75*, 2498–2501.
- (4) González, L. E.; González, D. J. *J. Phys.: Condens. Matter* **2006**, *18*, 11021–11030.
- (5) Cao, B.; Starace, A. K.; Judd, O. H.; Jarrold, M. F. *J. Am. Chem. Soc.* **2009**, *131*, 2446–2447.
- (6) Cao, B.; Starace, A. K.; Judd, O. H.; Bhattacharyya, I.; Jarrold, M. F.; Lopez, J. M.; Aguado, A. *J. Am. Chem. Soc.* **2010**, *132*, 12906–12918.
- (7) Schmidt, M.; Kusche, R.; Kronmüller, W.; von Issendorff, B.; Haberland, H. *Phys. Rev. Lett.* **1997**, *79*, 99–102.
- (8) Breaux, G. A.; Neal, C. M.; Cao, B.; Jarrold, M. F. *Phys. Rev. Lett.* **2005**, *94*, 173401.
- (9) Aguado, A.; Jarrold, M. F. *Annu. Rev. Phys. Chem.* **2001**, *62*, 151–172.
- (10) Pawlow, P. Z. *Phys. Chem.* **1909**, *65*, 1–35.
- (11) Starace, A. K.; Cao, B.; Judd, O. H.; Bhattacharyya, I.; Jarrold, M. F. *J. Chem. Phys.* **2010**, *132*, 034302.
- (12) Cao, B.; Starace, A. K.; Judd, O. H.; Jarrold, M. F. *J. Chem. Phys.* **2009**, *130*, 204303.
- (13) Berry, R. S. *Microscale Thermophys. Eng.* **1997**, *1*, 1–18.
- (14) Neal, C. M.; Starace, A. K.; Jarrold, M. F. *Phys. Rev. B* **2007**, *76*, 054113.
- (15) Starace, A. K.; Neal, C. M.; Cao, B.; Jarrold, M. F.; Aguado, A.; Lopez, J. M. *J. Chem. Phys.* **2008**, *129*, 144702.
- (16) Israelachvili, J. N.; McGuiggan, P. M.; Homola, A. M. *Science* **1988**, *240*, 189–191.

- (17) Kulkarni, B. S.; Krishnamurty, S.; Pal, S. J. *Phys. Chem. C* **2011**, *115*, 14615–14623.
- (18) Kojima, F.; Aida, T.; Inoue, S. *J. Am. Chem. Soc.* **1986**, *108*, 391–395.
- (19) Glockler, G. J. *Phys. Chem.* **1958**, *62*, 1049–1054.
- (20) Freund, H. J.; Messmer, R. P. *Surf. Sci.* **1986**, *172*, 1–30.
- (21) Freund, H. J.; Roberts, M. W. *Surf. Sci. Rep.* **1996**, *25*, 225–273.
- (22) Neal, C. M.; Starace, A. K.; Jarrold, M. F. *J. Am. Soc. Mass Spectrom.* **2007**, *18*, 74–81.
- (23) Neal, C. M.; Breaux, G. A.; Cao, B.; Starace, A. K.; Jarrold, M. F. *Rev. Sci. Instrum.* **2007**, *78*, 075108.
- (24) Hildenbrand, D. L. *Chem. Phys. Lett.* **1973**, *20*, 127–129.
- (25) Jarrold, M. F.; Bower, J. E. *J. Chem. Phys.* **1987**, *87*, 5728–5738.
- (26) Herman, Z.; Kerstetter, J.; Rose, T.; Wolfgang, R. *Discuss. Faraday Soc.* **1967**, *44*, 123–136.
- (27) Mahan, B. H.; Chiang, M. H.; Gislason, E. A.; Tsao, C. W.; Werner, A. S. *J. Phys. Chem.* **1971**, *75*, 1426–1437.
- (28) Kaiser, R. I.; Nguyen, T. L.; Mebel, A. M.; Lee, Y. T. *J. Chem. Phys.* **2002**, *116*, 1318–1324.
- (29) Carley, A. F.; Gallagher, D. E.; Roberts, M. W. *Spectrochim. Acta* **1987**, *43A*, 1447–1453.
- (30) Carley, A. F.; Gallagher, D. E.; Roberts, M. W. *Surf. Sci.* **1987**, *183*, L263–L268.
- (31) Hock, C.; Strassburg, S.; Haberland, H.; von Issendorff, B.; Aguado, A.; Schmidt, M. *Phys. Rev. Lett.* **2008**, *101*, 023401.